CHEMISTRY

Propane oxidative dehydrogenation over highly selective hexagonal boron nitride catalysts: The role of oxidative coupling of methyl

Jinshu Tian[1], Jiangqiao Tan[1], Mingliang Xu[1], Zhaoxia Zhang[1], Shaolong Wan[1], Shuai Wang[1], Jingdong Lin[1]*, Yong Wang[1,2]*

Hexagonal boron nitride (*h*-BN) catalyst has recently been reported to be highly selective in oxidative dehydrogenation of propane (ODHP) for olefin production. In addition to propene, ethylene also forms with much higher overall selectivities to C2-products than to C1-products. In this work, we report that the reaction pathways over the *h*-BN catalyst are different from the V-based catalysts in ODHP. Oxidative coupling reaction of methyl, an intermediate from the cleavage of C–C bond of propane, contributes to the high selectivities to C2-products, leading to more C2-products than C1-products over the *h*-BN catalyst. This work not only provides insight into the reaction mechanisms involved in ODHP over the boron-based catalysts but also sheds light on the selective oxidation of alkanes such as direct upgrading of methane via oxidative upgrading to ethylene or CH_xO_y on boron-based catalysts.

INTRODUCTION

Dehydrogenation of propane by either oxidative or nonoxidative approaches is essential to the on-purpose production of propene, a valuable and versatile chemical feedstock. Oxidative dehydrogenation of propane (ODHP) in the presence of O_2 faces the challenges of deep oxidation of propane and propene to CO_x (CO and CO_2), often resulting in loss of propene selectivity and yield (*1*, *2*). V-based catalysts have been widely studied in the ODHP with main side products of CO_x and negligible amount of C2-products (*3*–*5*). However, the boron-based catalysts recently reported for the ODHP show very low selectivity to CO_x and relatively higher selectivity to C2-products than to C1-products (C2/C1 > 2) (*6*–*9*). For example, at a propane conversion of 4.1%, C2- and C1-selectivities are 8.6 and 3.5% (C2/C1 > 2), respectively, as reported by Grant *et al.* (*9*). Huang *et al.* (*7*) also reported that the C2/C1 ratio is higher than 2 at a propane conversion of 12% at 520°C over the hexagonal boron nitride (*h*-BN) nanosheet.

The different C2-selectivities and C2/C1 ratios observed in the ODHP over the *h*-BN and the V-based catalysts imply that the reaction mechanism is different on these two types of catalysts. It is believed that ODHP over the *h*-BN catalyst has higher tendency toward the cleavage of only the first C–C bond of propane than that over the V-based catalysts, which results in a higher selectivity of ethylene (*10*). The relative reactivity of methyl formed via the C–C bond cleavage could also play important roles in affecting the product selectivity on V-based and *h*-BN catalysts. In the oxidative coupling of the methane reaction (OCM) (*11*–*13*), methyl is generated via the C-H cleavage of methane, followed by its oxidative reactions, which mainly include three reaction pathways: (i) conversion of methyl to C1-oxygenates (*14*), (ii) oxidation of methyl to form CO_x (*12*), and (iii) coupling of methyl to form the C2-products (*15*, *16*). Therefore, understanding the fate of methyl or elucidation of the reaction pathways of methyl is essential for the in-depth understanding of the reaction mechanisms involved in the ODHP process over the boron-based catalysts.

Here, the reaction pathways of methyl derived from the C–C bond cleavage in ODHP over the *h*-BN catalyst were systematically studied. Among these reaction pathways, the oxidative coupling of methyl to C2-products was found to result in a higher C2/C1 ratio (>2), contributing to the higher C2-selectivities over the *h*-BN catalyst in ODHP.

RESULTS AND DISCUSSION

Figure 1 (A and B) shows the influence of reaction temperature on the catalytic performance of ODHP over the *h*-BN and VO_x/γ-Al_2O_3 catalysts, respectively. On the *h*-BN catalyst, the main by-product is C2-products and its selectivity increases with increasing propane conversion (Fig. 1A). In addition, the selectivity to C_2H_4 over the *h*-BN catalyst is higher than that to C_2H_6, which can mainly be attributed to the cleavage of propane. On the contrary, the main by-products are CO_x (CO and CO_2), with a negligible amount of C2-products on the VO_x/γ-Al_2O_3 catalyst (Fig. 1B). The C1-products are much more prevalent than the C2-products over the VO_x/γ-Al_2O_3 catalyst, which is typical over the V-based catalysts due to the inevitable over-oxidation of alkanes (C numbers > 1) or olefins in ODHP (*17*). However, it is interesting that the C2-products (C_2H_4 and C_2H_6 shown in fig. S1) are much more prevalent than the C1-products (C2/C1 > 2) over the *h*-BN catalyst (Fig. 2). This is quite different from that over the VO_x/γ-Al_2O_3 catalyst (*6*, *9*), which showed a C2/C1 ratio of close to 0 (Fig. 2). The observation of a higher C2/C1 ratio (>2) is a general feature for the ODHP over the *h*-BN and boron-based catalysts (*7*, *9*) at low reaction temperatures, yet its origin remains unaddressed.

Because of the complexity of C1-products in ODHP, the C1-products should be carefully examined to draw a definitive conclusion. To exclude the potential contribution of coke formation on the catalyst to the loss of carbon, both the fresh and spent *h*-BN catalysts were studied using Raman spectroscopy. Except the B-N stretching vibration in *h*-BN (~1367 cm^{-1}) (*18*), no C-related peaks (1340 and 1604 cm^{-1}) were found on the spent *h*-BN catalyst (fig. S2) (*19*, *20*), indicating that there is no coke deposition on the spent *h*-BN catalyst.

[1]Department of Chemistry, College of Chemistry and Chemical Engineering, National Engineering Laboratory for Green Chemical Productions of Alcohols-Ethers-Esters, State Key Laboratory of Physical Chemistry of Solid Surfaces, Collaborative Innovation Center of Chemistry for Energy Materials, Xiamen University, Xiamen 361005, China. [2]Voiland School of Chemical Engineering and Bioengineering, Washington State University, Pullman, WA 99164, USA.
*Corresponding author. Email: jdlin@xmu.edu.cn (J.L.); yongwang@pnnl.gov (Y.W.)

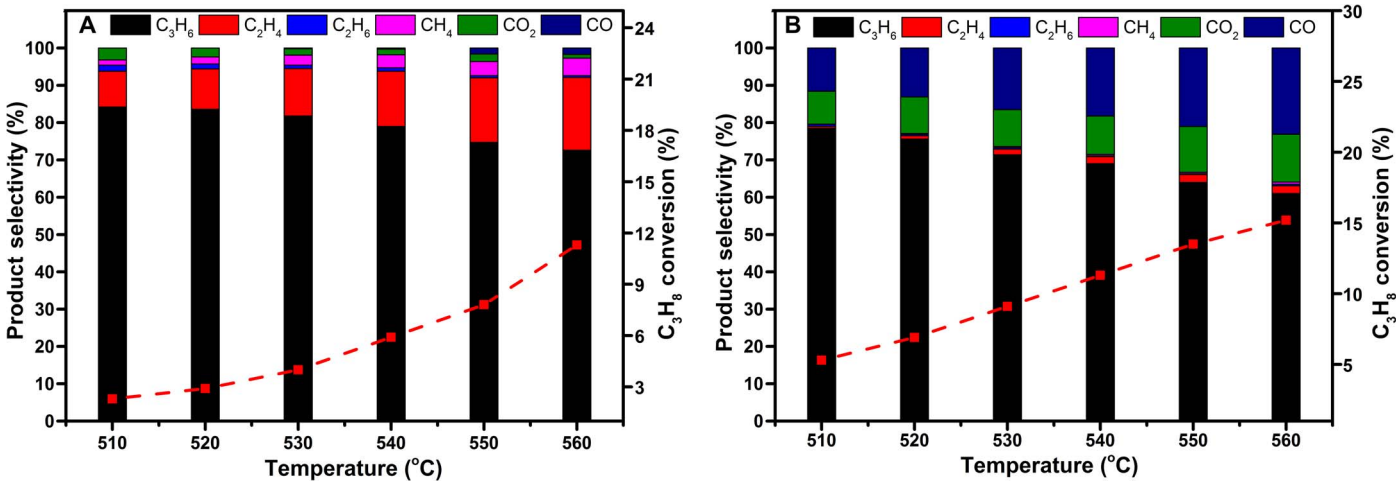

Fig. 1. The influence of reaction temperature on catalytic performance of ODHP. (**A**) *h*-BN catalyst; (**B**) $VO_x/\gamma\text{-}Al_2O_3$ catalyst.

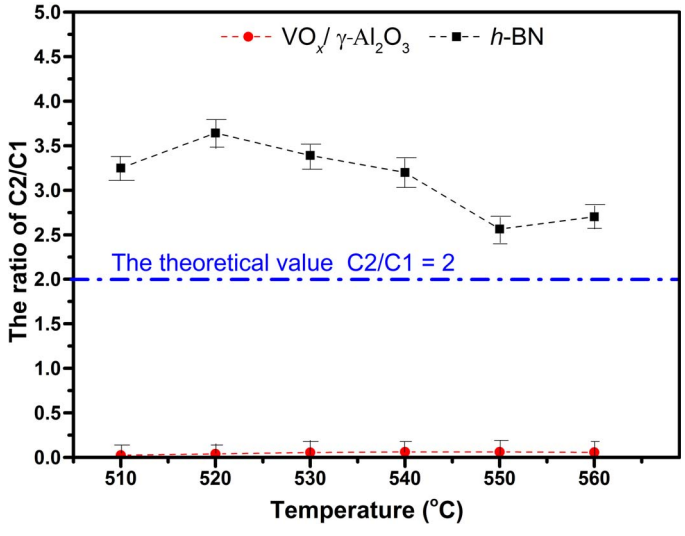

Fig. 2. Comparison of the C2/C1 ratio on the $VO_x/\gamma\text{-}Al_2O_3$ and *h*-BN catalysts at different reaction temperatures.

Table 1. The conversion and selectivity over the *h*-BN catalyst for ODHP at different reaction temperatures. $C_3H_8/O_2/He/N_2$ = 1:1:1:8; total flow rate, 33 ml/min. C1* indicates the total C1-products including CH_xO_y, CO_x, and CH_4. C3 indicates the selectivity to C_3H_6. C2 indicates the selectivity to C_2H_4 and C_2H_6.

Temperature (°C)	C_3H_8 conversion (%)	Selectivity (%)			
		C3	C2	C1*	C2/C1*
520	2.9	83.5	12.8	3.7	3.4
540	5.9	78.5	15.9	5.6	2.8
560	11.3	71.8	20.0	8.2	2.4

CO_x and CH_4 are the only C1-products detected on the V-based catalysts in ODHP, consistent with the reports elsewhere (*21*–*23*). On the *h*-BN catalysts, only CO_x and CH_4 have been reported as the C1-products so far (*8*, *9*, *24*–*26*). However, because of the higher tendency toward only the first C–C bond cleavage of propane over the *h*-BN catalysts compared to the V-based catalysts (*10*), methyl could thus be produced and the C1-products from the further conversion of methyl via oxidation, such as methanol and formaldehyde (CH_xO_y), could also be present. To confirm this, mass spectra signals of the products in ODHP over these two catalysts were collected (fig. S3). When the reaction temperature increases from room temperature to 600°C, CH_xO_y products (methanol and formaldehyde) gradually form and reach a maximum at 600°C over the *h*-BN catalyst. However, CH_xO_y products are negligible on the $VO_x/\gamma\text{-}Al_2O_3$ catalyst over the same range of temperatures studied. The formation of CH_xO_y on the *h*-BN catalyst was quantified and summarized in Table 1. Even considering CH_xO_y in the total C1-products, the C2/C1* ratio is still greater than 2. First, the C–C bond cleavage of propane is expected to form equal molar C1- and C2-products. Assuming that C2-products are not further converted to C1-products (by either continuous C–C bond cleavage or oxidation), the C2/C1 ratio should be at most 2. The fact that the C2/C1* ratio is greater than 2 on the *h*-BN catalyst (Table 1) suggests that there are other origins for the C2-products formation besides the cleavage of C–C bond in ODHP over the *h*-BN catalyst.

Ethylene is the main C2 by-product in ODHP over the *h*-BN catalyst, which is generally considered to originate from the C–C bond cleavage of propane (*10*). C2-products could also be formed in the presence of methyl via OCM as previously reported on the Mn_2O_3-Na_2WO_4/SiO_2 catalyst through the methyl oxidative reaction pathway (*15*). To investigate the possible involvement of OCM in the formation of C2-products on the *h*-BN catalyst, OCM experiments were conducted over the *h*-BN and $VO_x/\gamma\text{-}Al_2O_3$ catalysts at 600°C using a feed gas of $V(CH_4)/V(O_2)/V(N_2)$ = 1/1/1 (fig. S4). As shown in Fig. 3A, only CO_x products were detected over the $VO_x/\gamma\text{-}Al_2O_3$ catalyst at a methane conversion of 27.9%. However, both ethylene and ethane (almost 1:1) were also detected in addition to CO_x products over the *h*-BN catalyst, and C2-selectivities of 9% were reached at a methane

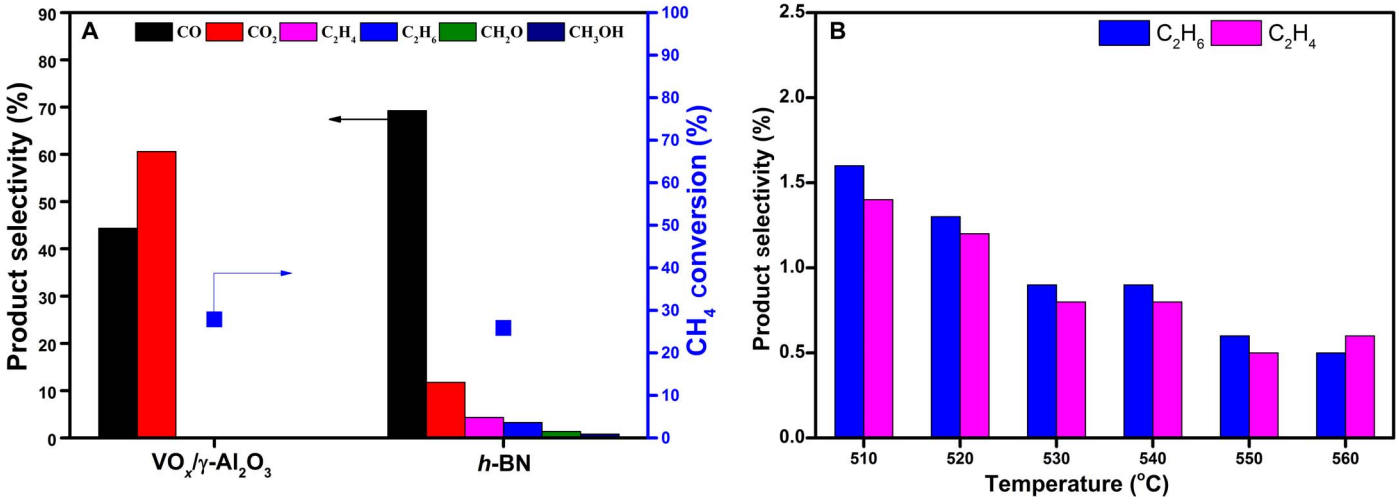

Fig. 3. The product distribution of OCM and ODHP over the VO_x/γ-Al_2O_3 and *h*-BN catalysts. (**A**) Conversion and selectivity of OCM over the VO_x/γ-Al_2O_3 and *h*-BN catalysts. (**B**) Selectivity to C2-products (C_2H_4 and C_2H_6) derived from the methyl coupling reaction in ODHP over the *h*-BN catalyst at different reaction temperatures.

conversion of 25.8% (Fig. 3A), which is similar to the recent report by Wang *et al.* (*27*). CH_xO_y also formed, with a selectivity of 2.1%. Apparently, under the same reaction conditions and at a similar methane conversion, the *h*-BN catalyst has noticeable OCM activity, while the VO_x/γ-Al_2O_3 catalyst has negligible OCM activity. Noting the similarity of the reaction pathways between OCM and oxidation of methyl, we can infer that the oxidative coupling of methyl to C2-products is involved in ODHP over the *h*-BN catalyst, which results in a higher C2-product selectivities. Experiments using ^{13}C-labeled propane also suggest that oxidative coupling of methyl is involved in ODHP on *h*-BN (fig. S5 and table S2). Collectively, the higher C_2H_4 selectivity and the C2/C1* ratio (>2) on the *h*-BN catalyst are due to both the C–C bond cleavage of propane to form ethyl followed by an additional C-H cleavage and the oxidative coupling of methyl on this catalyst. When we deducted C_2H_4 from those formed from the cleavage of C_3H_8, the selectivities to C_2H_4 and C_2H_6 derived from the methyl coupling reaction were similar (Fig. 3B).

To estimate the contribution of the oxidative coupling of methyl to the higher C2-product selectivities in ODHP, we first attempted to understand the origins of CO_x (main products of C1). CO_x may come from the oxidation of alkanes, olefins, and methyl in ODHP. Therefore, the oxidation reactions of propene, which is more reactive than ethylene, over the *h*-BN and VO_x/γ-Al_2O_3 catalysts were carried out. As shown in table S1, over-oxidation of propene readily occurs (about 99% CO_x selectivity) on the VO_x/γ-Al_2O_3 catalyst. However, there is only less than 1% conversion of propene over the *h*-BN catalyst even at a reaction temperature of 600°C. Because propene is known to be more reactive than ethylene, the fact that there is no over-oxidation of propene suggests that there is no direct over-oxidation of olefins over the *h*-BN catalyst in ODHP.

However, it is still uncertain whether the over-oxidation of alkanes (C_3H_8 and C_2H_6) occurs over the *h*-BN catalysts until now. Even so, we can conclude that C2/C1 will be less than 2 if the over-oxidation of C_{2+}(olefins/alkanes) does occur. Therefore, it is expected that C2/C1 will be equal or less than 2 in ODHP. When there is no over-oxidation of alkanes or olefins, the amount of C1-products should be equal to that of C2-products, assuming that there is no oxidative coupling of methyl occurring over the *h*-BN catalyst. In this case, the theoretical value of C1- or C2-selectivities (only cleavage of the first C–C bond) is defined using Eqs. 1 and 2 as below

$$\text{C1 (theoretical value)} = (100 - \text{C3})/3 \quad (1)$$

$$\text{C2 (theoretical value)} = (100 - \text{C3})^*(2/3) \quad (2)$$

where C1 or C2 represents the total selectivities of one- or two-carbon products, respectively, and C3 presents the selectivity of C_3H_6. The theoretical values of C1- and C2-selectivities as a function of temperature are shown in Fig. 4A, which are higher and lower than the measured C1- and C2-selectivities, respectively. Therefore, we can assume that the contribution of oxidative coupling of methyl is at least equal to the equation as below

$$\text{C2 (coupling reaction)} = (\text{C2} - 2^*\text{C1}^*)/3 \quad (3)$$

Therefore, the product distributions derived from methyl in ODHP over the *h*-BN catalyst at different reaction temperatures are analyzed and shown in Fig. 4B. These products are likely due to the following reaction pathways of methyl in ODHP over the *h*-BN catalyst: (i) CH_4 formation from methyl hydrogenation, (ii) oxidation of methyl to form CO_x or CH_xO_y, and (iii) oxidative coupling of methyl to produce the C2-products. The detailed selectivities of C2-products (C_2H_4 and C_2H_6) from the methyl coupling reaction are shown in Fig. 3B. The selectivities to C_2H_4 and C_2H_6 derived from the methyl coupling reaction in ODHP are almost similar to those derived from the methane coupling reaction (*27*), indicating that the C_2H_4 formation is via the CH_3* coupling reaction to form C_2H_6 followed by subsequent dehydrogenation to C_2H_4. From Fig. 4B, we can see that high temperature favors the formation of CO_x, CH_4, and CH_xO_y but disfavors C2-products from oxidative coupling (figs. S6 and S7), which is consistent with previous reports (*28*–*30*). When the reaction temperature further increases to higher than 570°C, the C2/C1 ratio is less than 2, which is possibly due to the inevitable over-oxidation of alkanes or olefins (fig. S8).

On the basis of the above results and discussions, the possible reaction pathways of ODHP over the *h*-BN catalyst are proposed and shown

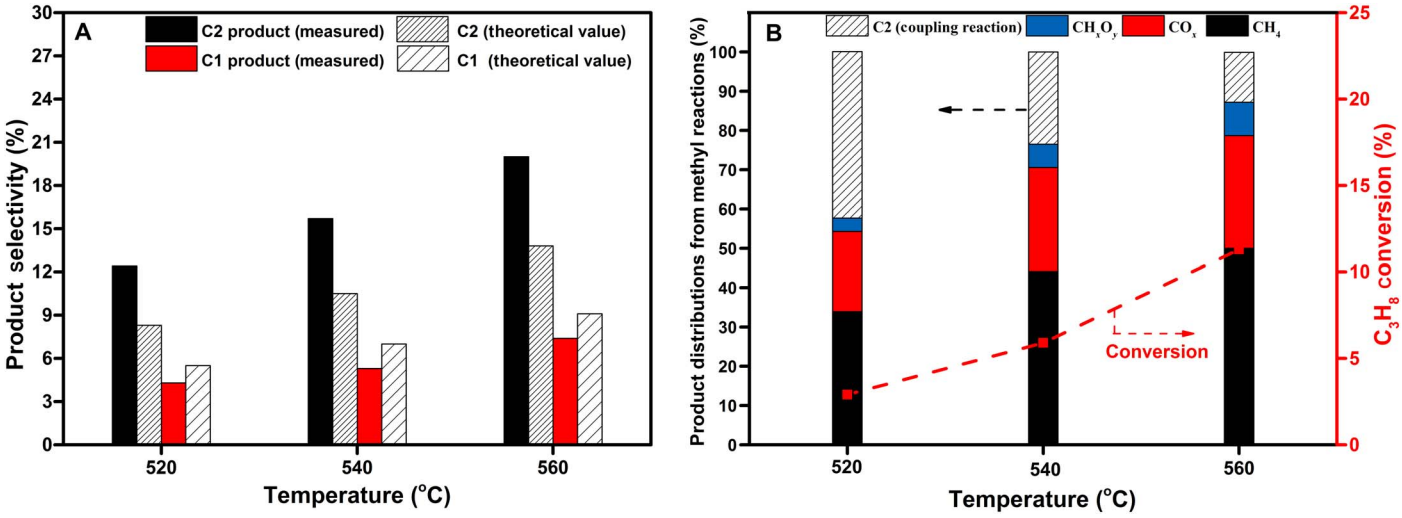

Fig. 4. The quantitative analysis of product from methyl reactions in ODHP over the *h*-BN catalyst. (**A**) Theoretical and measured selectivities of total C1- and C2-products. (**B**) Product distributions from methyl reactions in ODHP over the *h*-BN catalyst at different reaction temperatures.

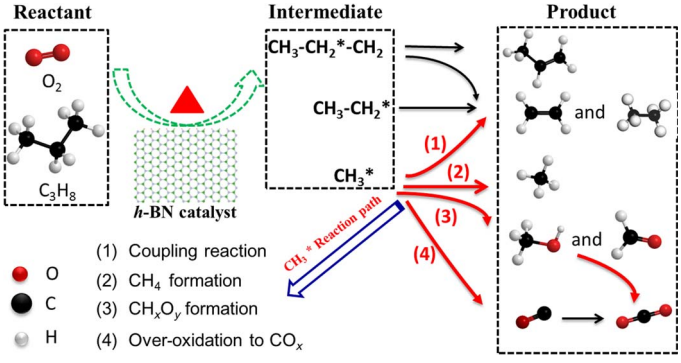

Fig. 5. The proposed reaction pathways of ODHP over the *h*-BN catalyst [using a structure model by Shi *et al.* (*31*) as an example].

in Fig. 5. Both C–H and first C–C bonds of propane are cleaved to form CH_3CH_2*CH_2, CH_3CH_2*, and CH_3* radicals over the *h*-BN surface. The CH_3CH_2*CH_2 radical (*6*) will continue dehydrogenation to form C_3H_6 and may also cleave to form CH_3CH_2* radicals. Meanwhile, C_2H_4 is generated from CH_3CH_2* as a main pathway to form the C2-products (mainly from the cleavage of propane). The methyl formed from the first C–C bond cleavage of propane could proceed via four reaction pathways: (i) oxidative coupling to form C2-products, (ii) hydrogenation to form CH_4, (iii) selective oxidation to form CH_xO_y, and (iv) over-oxidation to form CO_x. Among these reaction pathways, oxidative coupling of methyl makes additional contribution to C2-product selectivity in ODHP, leading to more C2-products than C1-products over the *h*-BN catalyst.

In summary, we report the understanding of reaction pathways in ODHP over the *h*-BN catalyst, which involve methyl generated from the C–C bond cleavage. Compared with the VO_x/γ-Al_2O_3 catalyst, there are four secondary reaction pathways involving methyl, i.e., methyl hydrogenation to form CH_4, methyl oxidation to produce CO_x and CH_xO_y, and oxidative coupling of methyl to produce C2-products. Besides the C–C bond cleavage of propane, part of C2-products is formed from the oxidative coupling of methyl in ODHP, which results in a higher C2/C1 ratio (>2) over the *h*-BN catalyst. This work not only provides further insight into the reaction mechanism of ODHP over the boron-based catalysts but also may broaden its application to other related upgrading reactions on light alkanes, such as selective oxidation of methane to ethylene or CH_xO_y.

MATERIALS AND METHODS

Materials

h-BN was commercially available from Qinhuangdao Eno High-Tech Material Development Co. Ltd., with a purity of >99%. The sample was used as provided without further chemical or thermal treatment. The *h*-BN catalysts before and after the reaction were named as *h*-BN fresh and *h*-BN spent, respectively.

As a comparison, 5 weight % (wt %) VO_x/γ-Al_2O_3 catalyst was prepared by wet impregnation (*23*). One gram of γ-Al_2O_3 support was impregnated with 5.7 ml of 0.1 M NH_4VO_3 solution, and the resultant slurry was stirred at room temperature for 12 hours. After the impregnation, the catalyst was dried at 90°C overnight and then calcined at 600°C for 4 hours. VO_x/γ-Al_2O_3 (5 wt %) was denoted as VO_x/γ-Al_2O_3.

Catalytic activity measurements

The VO_x/γ-Al_2O_3 and *h*-BN (80 to 100 mesh) catalysts were tested in a fixed-bed reactor with an inner diameter of 6 mm under atmospheric pressure. The flow rates of pure propane (or propene, methane) and mixture gas (O_2:N_2:He = 1:8:1) were controlled using two mass flow controllers (Sevenstar) and calibrated to each individual gas to allow a total flow rate of 33 ml/min (C_3H_8:O_2:N_2:He = 1:1:8:1). The reaction temperatures were set from 510° to 600°C. The reaction products were analyzed using a gas chromatograph (GC2060, Shanghai Ruimin GC Instruments Inc.) with a flame ionization detector [KB-Al_2O_3/Na_2SO_4 column for hydrocarbon (C_xH_y) measurement] and two thermal conductivity detectors (equipped with TDX-01 column for CO and CO_2 measurements and Porapak Q column for methanol and formaldehyde measurements for OCM). Experiments with quartz showed that the reaction conversion was negligible without the catalyst. The carbon balance was checked by comparing the number of moles of carbon in the outlet

stream to the number of moles of carbon in the feed. Under the typical evaluating conditions, the carbon balance was within 100 ± 4%. To account for the volume expansion in the reaction, helium was used as the internal standard. C_3H_8 conversion (X) and product selectivity (S) were calculated using the standard normalization method based on carbon atom balance and were defined as follows.

$$C_{\text{balance}} = \frac{\left(\sum N_i A_i f_i\right)_{\text{in}}}{\left(\sum N_i A_i f_i\right)_{\text{out}}}$$

$$X_{si}(\%) = \frac{\sum N_{pi} A_{pi} f_{pi}}{\sum N_{si} A_{si} f_{si} + \sum N_{pi} A_{pi} f_{pi}} * 100$$

$$S_{pj}(\%) = \frac{N_{pi} A_{pi} f_{pi}}{\sum N_{pi} A_{pi} f_{pi}} * 100$$

$$\text{GHSV}(\text{h}^{-1}) = F_{\text{total}} / V_{\text{cat}}$$

where s or p represents the reactant or product; i represents random gas in this reaction system; A_i and f_i are the chromatographic peak area and the calibration factor, respectively, of species i; V_{cat} is the volume of the catalyst loaded in the reactor (ml); F_{total} is the total flow of all inlet gas (ml/min); and N is the number of carbon atoms of the component.

Characterizations

A thermal gravimetric analyzer (TG 209F1, Netzsch, Germany) was used to investigate the carbon deposition of the spent catalysts. The samples were preheated at 80°C and then heated to 970°C at a rate of 10°C/min in air (20 ml/min). Raman spectra were obtained on a Renishaw UV-vis RT 1000 Raman spectrometer with an excitation wavelength of 532 nm and a resolution of 6 cm^{-1}. The sample was pressed into a sheet with a thickness of 2 mm and observed in the Renishaw using a laser scanning confocal microscope.

The reaction products were also identified and quantified by an online mass spectrometer (Pfeiffer OmniStar GSD 320). The m/z (mass/charge ratio) signals of CO, CO_2, CH_3OH, and CH_2O were 28, 44, 31, and 30, respectively. The ODHP at reaction temperatures of 600°C was carried out, and the products were pumped into the mass spectrometer with m/z from 1 to 100.

^{13}C isotopic labeling experiments were performed in a fixed-bed single-pass flow reactor equipped with online mass spectrometry (MS). The details are described as below: A mixture of He and O_2 with 9:1 (O_2: 1 ml/min) passed the h-BN catalyst at 560°C until the baseline reached flat and then the ^{13}C-labeled propane (Cambridge Isotope Laboratories; 99%; 1 ml each time) was introduced into the flow using an injection syringe at specified temperatures (560°, 540°, 520°, and 510°C). The chemical and isotopic compositions of the reactor effluent were measured by online MS at intervals of 6 s with m/z from 24 to 32.

SUPPLEMENTARY MATERIALS

Supplementary material for this article is available at http://advances.sciencemag.org/cgi/content/full/5/3/eaav8063/DC1

Supplementary Text

Fig. S1. Product selectivities to C1 (CO_x and CH_4) and C2 (C_2H_4 and C_2H_6) in ODHP over the h-BN catalyst at different reaction temperatures.

Fig. S2. Characterizations of the fresh and spent h-BN catalysts.

Fig. S3. Mass spectral signals of the products in ODHP at different reaction temperatures.

Fig. S4. Schematic diagram of OCM process.

Fig. S5. Mass spectral signals of m/z in ODHP with isotopic pulsing experiments over h-BN.

Fig. S6. Distribution of partial products in ODHP over the h-BN catalyst at different reaction temperatures.

Fig. S7. Reaction pathways of methyl over the h-BN catalyst at different reaction temperatures.

Fig. S8. Comparison of C2/C1 ratio on the VO_x/γ-Al_2O_3 and h-BN catalysts at different reaction temperatures.

Table S1. Conversion and selectivity of propene oxidation over the VO_x/γ-Al_2O_3 and h-BN catalysts.

Table S2. ^{13}C-labeled propane and possible products from ODHP.

Reference (*32*)

REFERENCES AND NOTES

1. R. Grabowski, Kinetics of oxidative dehydrogenation of C_2-C_3 alkanes on oxide catalysts. *Catal. Rev.* **48**, 199–268 (2006).
2. C. A. Carrero, R. Schlögl, I. E. Wachs, R. Schomäcker, Critical literature review of the kinetics for the oxidative dehydrogenation of propane over well-defined supported vanadium oxide catalysts. *ACS Catal.* **4**, 3357–3380 (2014).
3. S. A. Karakoulia, K. S. Triantafyllidis, G. Tsilomelekis, S. Boghosian, A. A. Lemonidou, Propane oxidative dehydrogenation over vanadia catalysts supported on mesoporous silicas with varying pore structure and size. *Catal. Today* **141**, 245–253 (2009).
4. C. L. Pieck, M. A. Bañares, J. L. G. Fierro, Propane oxidative dehydrogenation on VO_x/ZrO_2 catalysts. *J. Catal.* **224**, 1–7 (2004).
5. S. Barman, N. Maity, K. Bhatte, S. Ould-Chikh, O. Dachwald, C. Haeßner, Y. Saih, E. Abou-Hamad, I. Llorens, J.-L. Hazemann, K. Köhler, V. D'Elia, J.-M. Basset, Single-site VO_x moieties generated on silica by surface organometallic chemistry: A way to enhance the catalytic activity in the oxidative dehydrogenation of propane. *ACS Catal.* **6**, 5908–5921 (2016).
6. J. T. Grant, C. A. Carrero, F. Goeltl, J. Venegas, P. Mueller, S. P. Burt, S. E. Specht, W. P. McDermott, A. Chieregato, I. Hermans, Selective oxidative dehydrogenation of propane to propene using boron nitride catalysts. *Science* **354**, 1570–1573 (2016).
7. R. Huang, D. Su, C. Liang, "Catalytic conversion of light paraffins into olefins over metal-free catalysts," thesis, Dalian University of Technology, Dalian, China (2015).
8. L. Shi, D. Wang, W. Song, D. Shao, W.-P. Zhang, A.-H. Lu, Edge-hydroxylated boron nitride for oxidative dehydrogenation of propane to propylene. *ChemCatChem* **9**, 1788–1793 (2017).
9. J. T. Grant, W. P. McDermott, J. M. Venegas, S. P. Burt, J. Micka, S. P. Phivilay, C. A. Carrero, I. Hermans, Boron and boron-containing catalysts for the oxidative dehydrogenation of propane. *ChemCatChem* **9**, 3623–3626 (2017).
10. J. M. Venegas, J. T. Grant, W. P. McDermott, S. P. Burt, J. Micka, C. A. Carrero, I. Hermans, Selective oxidation of *n*-butane and isobutane catalyzed by boron nitride. *ChemCatChem* **9**, 2118–2127 (2017).
11. S. Pak, C. E. Smith, M. P. Rosynek, J. H. Lunsford, Conversion of methyl radicals to methanol and formaldehyde over vanadium oxide catalysts. *J. Catal.* **165**, 73–79 (1997).
12. S. Pengpanich, V. Meeyoo, T. Rirksomboon, K. Bunyakiat, Catalytic oxidation of methane over CeO_2-ZrO_2 mixed oxide solid solution catalysts prepared via urea hydrolysis. *Appl. Catal. A* **234**, 221–233 (2002).
13. P. Schwach, X. Pan, X. Bao, Direct conversion of methane to value-added chemicals over heterogeneous catalysts: Challenges and prospects. *Chem. Rev.* **117**, 8497–8520 (2017).
14. J. A. Barbero, M. C. Alvarez, M. A. Bañares, M. A. Peña, J. L. G. Fierro, Breakthrough in the direct conversion of methane into c_1-oxygenates. *Chem. Commun.* **11**, 1184–1185 (2002).
15. P. Wang, G. Zhao, Y. Wang, Y. Lu, $MnTiO_3$-driven low-temperature oxidative coupling of methane over TiO_2-doped Mn_2O_3-Na_2WO_4/SiO_2 catalyst. *Sci. Adv.* **3**, 1–9 (2017).
16. V. Fleischer, R. Steuer, S. Parishan, R. Schomäcker, Investigation of the surface reaction network of the oxidative coupling of methane over $Na_2WO_4/Mn/SiO_2$ catalyst by temperature programmed and dynamic experiments. *J. Catal.* **341**, 91–103 (2016).
17. A. A. Lemonidou, L. Nalbandian, I. A. Vasalos, Oxidative dehydrogenation of propane over vanadium oxide based catalysts: Effect of support and alkali promoter. *Catal. Today* **61**, 333–341 (2000).
18. R. Huang, B. Zhang, J. Wang, K.-H. Wu, W. Shi, Y. Zhang, Y. Liu, A. Zheng, R. Schlögl, D. S. Su, Direct insight into ethane oxidative dehydrogenation over boron nitrides. *ChemCatChem* **9**, 3293–3297 (2017).
19. B. M. Vogelaar, A. D. van Langeveld, S. Eijsbouts, J. A. Moulijn, Analysis of coke deposition profiles in commercial spent hydroprocessing catalysts using Raman spectroscopy. *Fuel* **86**, 1122–1129 (2007).
20. H. Xiong, S. Lin, J. Goetze, P. Pletcher, H. Guo, L. Kovarik, K. Artyushkova, B. M. Weckhuysen, A. K. Datye, Thermally stable and regenerable platinum-tin clusters

for propane dehydrogenation prepared by atom trapping on ceria. *Angew. Chem. Int. Ed.* **56**, 8986–8991 (2017).
21. O. V. Buyevskaya, M. Baerns, Catalytic selective oxidation of propane. *Catal. Today* **42**, 315–323 (1998).
22. W.-D. Zhang, C.-T. Au, H.-L. Wan, The active phase and support effect on V_2O_5/Y_2O_3 catalysts for propane oxidative dehydrogenation. *Appl. Catal. A* **181**, 63–69 (1999).
23. A. A. Ayandiran, I. A. Bakare, H. Binous, S. Al-Ghamdi, S. A. Razzak, M. M. Hossain, Oxidative dehydrogenation of propane to propylene over $VO_x/CaO/\gamma\text{-}Al_2O_3$ using lattice oxygen. *Catal. Sci. Technol.* **6**, 5154–5167 (2016).
24. F. Jiao, J. Li, X. Pan, J. Xiao, H. Li, H. Ma, M. Wei, Y. Pan, Z. Zhou, M. Li, S. Miao, J. Li, Y. Zhu, D. Xiao, T. He, J. Yang, F. Qi, Q. Fu, X. Bao, Selective conversion of syngas to light olefins. *Science* **351**, 1065–1068 (2016).
25. F. Guo, P. Yang, Z. Pan, X.-N. Cao, Z. Xie, X. Wang, Carbon-Doped BN Nanosheets for the oxidative dehydrogenation of ethylbenzene. *Angew. Chem. Int. Ed.* **56**, 8231–8235 (2017).
26. Y. Fang, X. Wang, Metal-free boron-containing heterogeneous catalysts. *Angew. Chem. Int. Ed.* **56**, 15506–15518 (2017).
27. Y. Wang, L. Zhao, L. Shi, J. Sheng, W. Zhang, X.-M. Cao, P. Hu, A.-H. Lu, Methane activation over a boron nitride catalyst driven by in situ formed molecular water. *Catal. Sci. Technol.* **8**, 2051–2055 (2018).
28. J. C. Mackie, Partial oxidation of methane: The role of the gas phase reactions. *Catal. Rev.* **33**, 169–240 (1991).
29. V. R. Choudhary, A. S. Mammon, S. D. Sansare, Selective oxidation of methane to CO and H_2 over Ni/MgO at low temperatures. *Angew. Chem. Int. Ed.* **31**, 1189–1190 (1992).
30. H. Berndt, A. Martin, A. Brückner, E. Schreier, D. Müller, H. Kosslick, G.-U. Wolf, B. Lücke, Structure and catalytic properties of VO_x/MCM materials for the partial oxidation of methane to formaldehyde. *J. Catal.* **191**, 384–400 (2000).
31. L. Shi, Y. Wang, B. Yan, W. Song, D. Shao, A.-H. Lu, Progress in selective oxidative dehydrogenation of light alkanes to olefins promoted by boron nitride catalysts. *Chem. Commun.* **54**, 10936–10946 (2018).
32. K. Takanabe, E. Iglesia, Rate and selectivity enhancements mediated by OH radicals in the oxidative coupling of methane catalyzed by $Mn/Na_2WO_4/SiO_2$. *Angew. Chem. Int. Ed.* **47**, 7689–7693 (2008).

Acknowledgments: We thank F. Lin and J. Zheng (Pacific Northwest National Laboratory, USA) for assistance on MS measurements. **Funding:** This work was supported by the National Natural Science Foundation of China (grants 21576227, 91545114, 91545203, and 21673189) and the Fundamental Research Funds for the Central Universities (grant 20720160032). **Author contributions:** J.L. and Y.W. conceived the idea for the project. J. Ti. and M.X. conducted the material synthesis. J. Ti. and J. Ta. performed the structural characterizations and catalytic test. J.L., Y.W., and J. Ti. discussed the catalytic results. J. Ti. drafted the manuscript under the guidance of Y.W. All authors discussed and commented on the manuscript. **Competing interests:** The authors declare that they have no competing interests. **Data and materials availability:** All data needed to evaluate the conclusions in the paper are present in the paper and/or the Supplementary Materials. Additional data related to this paper may be requested from the authors.

Submitted 22 October 2018
Accepted 30 January 2019
Published 15 March 2019
10.1126/sciadv.aav8063

Citation: J. Tian, J. Tan, M. Xu, Z. Zhang, S. Wan, S. Wang, J. Lin, Y. Wang, Propane oxidative dehydrogenation over highly selective hexagonal boron nitride catalysts: The role of oxidative coupling of methyl. *Sci. Adv.* **5**, eaav8063 (2019).

Science Advances

Propane oxidative dehydrogenation over highly selective hexagonal boron nitride catalysts: The role of oxidative coupling of methyl

Jinshu Tian, Jiangqiao Tan, Mingliang Xu, Zhaoxia Zhang, Shaolong Wan, Shuai Wang, Jingdong Lin and Yong Wang

Sci Adv **5** (3), eaav8063.
DOI: 10.1126/sciadv.aav8063